Physica B 695 (2024) 416492

Contents lists available at ScienceDirect

Physica B: Condensed Matter

journal homepage: www.elsevier.com/locate/physb

Investigation on the structural, elastic, electronic, thermodynamic, and vibrational properties of the full heusler Sc_2XAl (X =Cd and Zn): An ab initio study

Nihat Arıkan [a], Osman Örnek [b], Ahmet İyigör [c], Murat Çanlı [d,*]

[a] Department of Medical Services and Techniques, University of Osmaniye Korkut Ata, Osmaniye, Turkiye
[b] Department of Materials and Metallurgical Engineering, University of Kirsehir Ahi Evran, Kirsehir, Turkiye
[c] Department of Machine and Metal Technologies, University of Kirsehir Ahi Evran, Kirsehir, Turkiye
[d] Department of Chemistry and Chemical Processing Technologies, University of Kirsehir Ahi Evran, 40500, Kirsehir, Turkiye

ARTICLE INFO

Keywords:
DFT
Ab initio
Elastic properties
Electronic band structure
Phonon
Thermodynamic properties

ABSTRACT

The structural, mechanical, electronic, thermodynamic, and phonon characteristics of Sc_2CdAl and Sc_2ZnAl in $L2_1$ phase were the main focuses on this investigation. The density of states (DOS) and electronic band spectra signify the metallic behavior of the $L2_1$ phase of both materials. The impact of atomic arrangement with respect to the Wyckoff sites on the mechanical stability were additionally studied. The elastic constants of Sc_2CdAl and Sc_2ZnAl alloys indicated that these alloys convened Born mechanical stability criteria. Using the density functional perturbation theory's first-principle linear response method, complete phonon spectra have been acquired. Moreover, the quasi-harmonic approximation, specific heat capacity at constant volume, the internal free energy, entropy, and vibrational free energy variations of Sc_2CdAl and Sc_2ZnAl as full Heusler alloys have been utilized in examination the change over the temperature between 0 and 800 K. Both alloys might find application in real industrial applications.

1. Introduction

Heusler alloys' many capabilities, such as thermoelectric, spintronics, shape memory, and a vast array of other capabilities, were made possible by changing the elements, which sparked a wide spectrum of interest like finding alternative energy sources to reduce environmental risks [1–6]. Four groupings might be used to classify Heusler alloys: (i) When Y has smaller valence number than X, full Heusler alloys with the chemical formulation X_2YZ crystallize in the $L2_1$ phase of the typical Heusler alloy with the prototype Cu_2MnAl. (ii) The inverse Heusler (XA), which crystallizes in the $C1_b$ phase with prototype Hg_2TiCu and has the full Heusler chemical formula only a higher valence number for Y than X. (iii) Half-Heusler alloys are crystalline in the $C1_b$ phase and contain the chemical formula XYZ, which is a full Heusler with one X absent. (iv) Quaternary Heusler alloys are crystalline in the LiMgPdSn-type and comprise the chemical formula XX'YZ. Numerous prior investigations employing a range of computational and experimental methodologies have focused on Heusler alloys [4–6]. Research on 171 complete Heusler compounds based on scandium was conducted in 2019 by Han et al. [7]. They listed the energy difference $\left(\Delta E = E_{XA}^{total} - E_{L2_1}^{total}\right)$ between the two structures. For Sc_2CdAl and Sc_2ZnAl alloys, they determined that since ΔE is larger than zero, the $L2_1$ structure is more stable. It follows that there is a greater chance of synthesizing the $L2_1$ structure. Additionally, they used ab initio simulations to determine the electrical band structure of the alloys mentioned here.

The three subclasses of Heusler alloys, which are inverse, half, and quaternary Heusler alloys, have a crystalline structure that belongs to the F-43m (No. 216) space group. On the other hand, full Heusler alloys have a crystalline structure that belongs to the Fm-3m (No. 225) space group and adopts the $L2_1$ cubic structure, also known as the Cu_2MnAl-prototype. While "Y" and "Z" atoms are optimized at 4a (0, 0, 0) and 4b (1/2, 1/2, 1/2) Wyckoff locations, the "X" atom occupies at 8c (1/4, 1/4, 1/4) Wyckoff position [8,9]. X_2YZ type full-Heusler has been discovered to form several intermetallic classes [9] and has also found intriguing uses in thermoelectric devices [10]. Intermetallic alloys known as full Heusler alloys with the formula X_2YZ have Z as a main group metal having *sp* electrons, and X and Y as transition group metals. These alloys'

* Corresponding author.
E-mail address: murat.canli@ahievran.edu.tr (M. Çanlı).

https://doi.org/10.1016/j.physb.2024.416492
Received 4 August 2024; Received in revised form 29 August 2024; Accepted 2 September 2024
Available online 3 September 2024

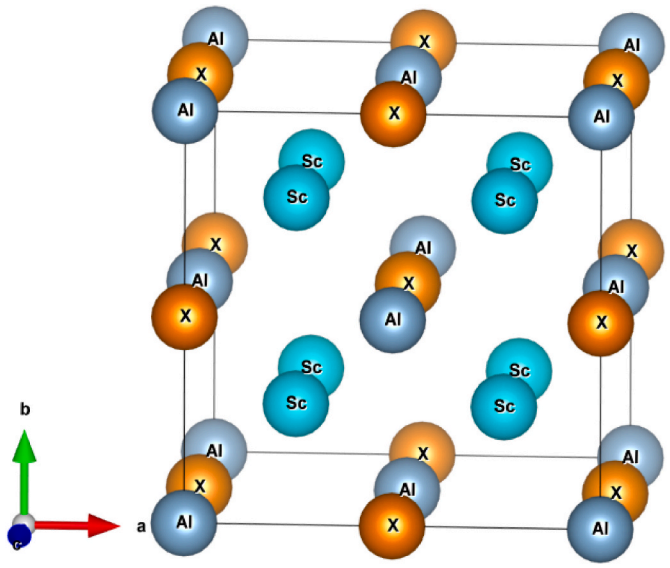

Fig. 1. Unit cell of Sc_2XAl compounds.

intriguing characteristics, which include structural, electronic, magnetic, mechanical, thermoelectric, and lattice dynamics, have drawn a lot of interest due to their high electrical conductivity, making them ideal for spintronics [11–16]. The characteristics and possible uses of metallic full Heusler alloys have been examined in earlier research [17–21]. These investigations show that metallic full Heusler alloys are becoming more and more popular due to their wide range of possible uses. Sc based full Heusler alloys have showed zero energy band gaps in a previous work [12]. This quality allows the use of similar alloys as semiconductor. Counting the total valence electrons of any Heusler alloy might straightforwardly help to predict its electronic and magnetic properties [11]. The elastic properties of materials are important because they provide an elaborate understanding of various fundamental physical properties like the stability and stiffness of the materials against externally applied stresses [22–24].

In this study, the main subject of our investigation is to present detailed ab initio calculations on the Sc_2CdAl and Sc_2ZnAl full-Heusler alloys that many of their physical characteristics are still unknown, despite the likelihood of few theoretical improvements in this area. Here, we have thoroughly described their mechanical and lattice dynamic characteristics. The entire phonon spectra and elastic characteristics of herein investigated full-Heusler alloys have not been planned on any previous theoretical or experimental technique or available data. We have also revealed and projected the structural, electrical, elastic, thermodynamic, and vibration characteristics of Sc_2CdAl and Sc_2ZnAl in the $L2_1$ phase, respectively.

2. Method of calculations

Using the Quantum Espresso code's first principles plane wave pseudopotential approach, the calculations for the alloys Sc_2CdAl and Sc_2ZnAl were carried out [25,26]. The affection of the nuclei, electron-electron interactions with each other was intended using the projector augmented wave (PAW) based pseudopotential. Using the generalized gradient approximation (GGA) parameterized by Perdew, Burke, and Ernzerhof (PBE) [27], the electronic exchange correlation potentials were handled. The cut-offs were calculated for charge density and wave functions as 550 Ry and 55 Ry, respectively. 10^{-9} Ry was selected as the convergence level, with a mixing beta of 0.7 to get accurate outcomes. The energy convergence criterion of 1 mRy per atom is supplied via self-consistent solutions of the Kohn-Sham equations [28] employing Monkhorst-Pack specific k-points of $10 \times 10 \times 10$ [29] in the Brillouin region. Following the utilization of Kohn-Sham equations, lattice dynamic characteristics were ascertained within the context of self-consistent density functional perturbation theory [30,31]. Dynamic matrices in arbitrary wave vectors were employed on a $4 \times 4 \times 4$ q-points mesh and an inverse Fourier transform was conducted in this mesh to calculate the exact phonon distributions and vibrational density of the states. Additionally, the Gibbs2 algorithm with quasi-harmonic approximation (QHA) was exercised to determine the thermodynamic characteristics under constant volume C_v. Applying the energy-strain approach in the thermo-pw code allowed for the extraction of elastic and thermodynamic parameters. The polycrystalline elastic parameters were used to relate the stress to strain with using Poisson's (σ) ratio, bulk modulus (B), shear modulus (G), Young's modulus(E), Debye temperature (θ_D), and anisotropy factor (A) in terms of the symmetry elements (Cij) [23].

3. Results and discussion

The crystal structure of the full Heusler alloys Sc_2CdAl and Sc_2ZnAl is indicated in Fig. 1. Besides load deflection, thermoelastic stress, internal strain, sound velocities and fracture toughness, interatomic bonding, equations of state, and phonon spectra are several fundamental solid-state phenomena that need elastic properties to understand specific heat, thermal expansion, and Debye temperature [24,32]. The efficiency of external forces on the crystal can be understood by the relation of proportionality coefficients Cij with applied strain.

The materials under investigation are cubic phase and belong to the Fm $\overline{3}$ m space group (#225). The numbers for the lattice parameters, bulk modulus and elastic constants of the assessed alloys have been displayed in Table 1. Upon comparing the lattice constants' values with those reported in theoretical studies, it was found that the Sc_2CdAl alloy exhibited a discrepancy of approximately 0.5 %, while the Sc_2ZnAl alloy showed a discrepancy ranging from 0.01 % to 0.4 %. Based on these results, the estimated lattice values for both alloys show excellent agreement when compared to currently available data from the literature [7,33,34]. It is understood that Sc_2CdAl has a higher lattice constant due to the relatively higher atomic radius of Cd. Sc_2ZnAl alloy is the less compressible among the alloys studied because, in contrast to the behavior of the lattice constant, the bulk modulus increased as the atomic number of the Zn atom decreased.

In addition, any material's resistance to shear stress can be predicted by its shear modulus (G). G is also known as the modulus of hardness and explains how shear force and shear stress are related to each other

Table 1
Lattice parameters, bulk moduli, shear moduli and elastic constants of the alloys.

Materials	References	a_0 (Å)	*B (GPa)*	*G(GPa)*	*B/G*	C_{11} *(GPa)*	C_{12} *(GPa)*	C_{44} *(GPa)*
Sc_2CdAl	This work	6.915	75.201	35.746	2.103	90.838	67.352	71.923
	Theory [7]	6.950	73	37	1.972	96	78	67
	Theory [30]	6.879						
	Theory [29]	6.949						
Sc_2ZnAl	This work	6.720	78.817	45.826	1.719	103.244	66.603	83.164
	Theory [7]	6.740	76	46	1.652	102	63	80
	Theory [30]	6.721						
	Theory [29]	6.749						

Table 2
The formation energy, young moduli, anisotropy factor, Poisson's ratio, microhardness parameter, melting point, Kleinman parameter, Debye temperature, stiffness parameter of both alloys computed by different theories.

Material	References	ΔE	E (GPa)	A	σ	H_v	T_m	ζ	$\theta_D(K)$	C'
Sc_2CdAl	This work	−0.366	91.313	6.124	0.270	5.512	958.064	0.817	317.168	11.743
	Theory [7]	–	–	3.80	0.27				–	–
	Theory [29]	−0.387								
	Theory [30]	−0.379								
Sc_2ZnAl	This work	−0.426	114.188	4.539	0.24	7.98	1024.499	0.734	401.544	18.320
	Theory [7]	–	–	2.28	0.25				–	–
	Theory [29]	−0.425								
	Theory [30]	−0.428								

within the elastic limit of the material. Shear modulus values confirmed the other theoretical calculation results for both Sc_2CdAl and Sc_2ZnAl as shown in Table 1. Sc_2CdAl has 35.746 GPa in present study while it was 37 GPa in Han et al.'s work [7]. Similarly, for Sc_2ZnAl it was determined as 45.826 GPa and 46 GPa in this study and another study [7], respectively. Shear modulus (G) is the resistance of the material to a shape change under shearing force.

Bulk modulus helps to understand a material's resistance level to compression. Bulk modulus also shows the relationship between compressive stress and volumetric strain within a material's elastic limit. The estimated critical value of Poisson's ratio is known as 0.26 GPa. Materials having values over 0.26 for Poisson's ratios are expected to lose their ductility whereas materials with Poisson's ratios lower than 0.26 are more likely to fracture. For Sc_2CdAl and Sc_2ZnAl alloys, the estimated Poisson's ratios were found to be 0.27 and 0.24, respectively, which are coherent with the current theoretical data. In general, the values indicate that Sc_2CdAl is ductile and Sc_2ZnAl is brittle nature. Dividing a material's bulk modulus with its shear modulus leads to find out Pugh ratio being a dimensionless constant. In general, materials with low B/G (Pugh ratio) values are brittle. Any value over the critical value for B/G which is 1.75 denotes ductility in the material, whereas a number below it shows brittleness. Pugh ratios for Sc_2CdAl and Sc_2ZnAl are estimated to be 2.103 and 1.719, respectively, according to Table 1. In general, the values indicate that Sc_2CdAl is ductile and Sc_2ZnAl is brittle.

The mechanical stability, machinability index, ductile-brittle behavior, stiffness, and hardness of a material are indicated by the elastic constant (Cij) which are shortly displayed in Table 1. The ease with which a material may be machined using conventional methods is measured by its machinability. The machinability of a material is greatly influenced by factors including its ductility, strength, hardness, and thermal conductivity. A material's machinability index, or μM, can be written as follows in Equation (1):

$$\mu M = \frac{B}{C_{44}F} \tag{1}$$

The calculated μM values for Sc_2CdAl and Sc_2ZnAl are 1.045 and 0.947, respectively. The alloys under investigation have a rather high machinability index (μM).

C_{11}, C_{12} and C_{44} as three symmetry elements in cubic alloys were computed to find out the stability. For a system to be mechanically stable, it must encounter the Born-Huang stability criteria as follows [12,35,36] (Equation (2)).

$$(C_{11} - C_{12}) > 0, (C_{11} + 2C_{12}) > 0, C_{11} > 0, C_{44} > 0, C_{12} < B < C_{11} \tag{2}$$

The mechanical stability of both materials satisfies the previously stated Born stability conditions in terms of the elastic constants. The C_{11} determines a material's resistance to principal strain based on its crystallographic orientations. On the other hand, the elastic constant C_{44} represents the material's resistance to shear deformation. Although C_{12} doesn't have a strictly physical significance, its conjunction with C_{11} and C_{44} provides further details about how elastic materials behave. In this study, all elastic constants (C_{11}, C_{12}, C_{44}) for both alloys have met the stability criteria. The calculated C_{11}, C_{12}, C_{44} values for Sc_2CdAl are 90.838, 67.352 and 71.923 GPa, respectively. For Sc_2ZnAl, those numbers are 103.244, 66.603 and 83.164 GPa, respectively.

The computed results validate the mechanical stability of both alloys by meeting the defined Born stability criterion. C′, defined as the stiffness of the crystal, reflects its capacity to tolerate shear deformation brought on by shear force acting in the $[1\bar{1}0]$ direction within the (110) plane, has the following formula in Equation (3):

$$C' = \frac{C_{11} - C_{12}}{2} \tag{3}$$

Both alloys are thermodynamically stable due to shear constant values of C'>0. The data ascertained by these computations are shown in Table 2, where the bulk moduli, young moduli, shear moduli and Poisson's ratio were computed using the approximations of Voigt [37], Reuss [38], and Hill [39]. The Reuss approximation and the Voigt approximation respectively provide the lower bound and the higher bound. In general, data obtained using the Hill approximation are more in line with experimental findings. Voigt-Reuss-Hill (VRH) approximation to account for the polycrystalline elasticity of the compounds including bulk modulus, Poisson's ratio, Young's modulus, and shear modulus calculated as follows (Equations (4)–(7)):

$$B = B_V = B_R = \frac{C_{11} + 2C_{12}}{3} \tag{4}$$

$$E = \frac{9BG_V}{3B + G_V} \tag{5}$$

$$G_H = \frac{(G_V + G_R)}{2} \tag{6}$$

$$\sigma = \frac{3B - 2G}{2(3B + G)} \tag{7}$$

The estimated data for these terms by applying the equation mentioned above are shown in Table 2. The negative value of ΔE implies that Sc_2XAl prototype structures can easily be synthesized experimentally in both structures (Table 2). In addition, it is verified from ΔE that $L2_1$-type structure is the most stable phase. Young's modulus (E) represents the stiffness of a material showing against in reaction to compressive or tensile stress. E shows stress to strain in a material's elastic behavior.

Ductility nature of a material can be also exhibited by Kleinman parameter (ζ). It can be called as the internal strain parameter (ζ), commonly known as the internal strain parameter, is a measurement used to evaluate the bonding flexibility of the material against stretching and bending. It is represented by ζ and expressed as (Equation (8)):

$$\zeta = \frac{C11 + 8C12}{7C11 + 2C12} \tag{8}$$

It ranges between 0 and 1 that indicates the resistance to external pressure. Harrison developed a formula to determine ζ using elastic coefficients; Kleinman's work shows that ζ = 0 indicates bond bending and ζ = 1 indicates bond tension. Considering that for both materials,

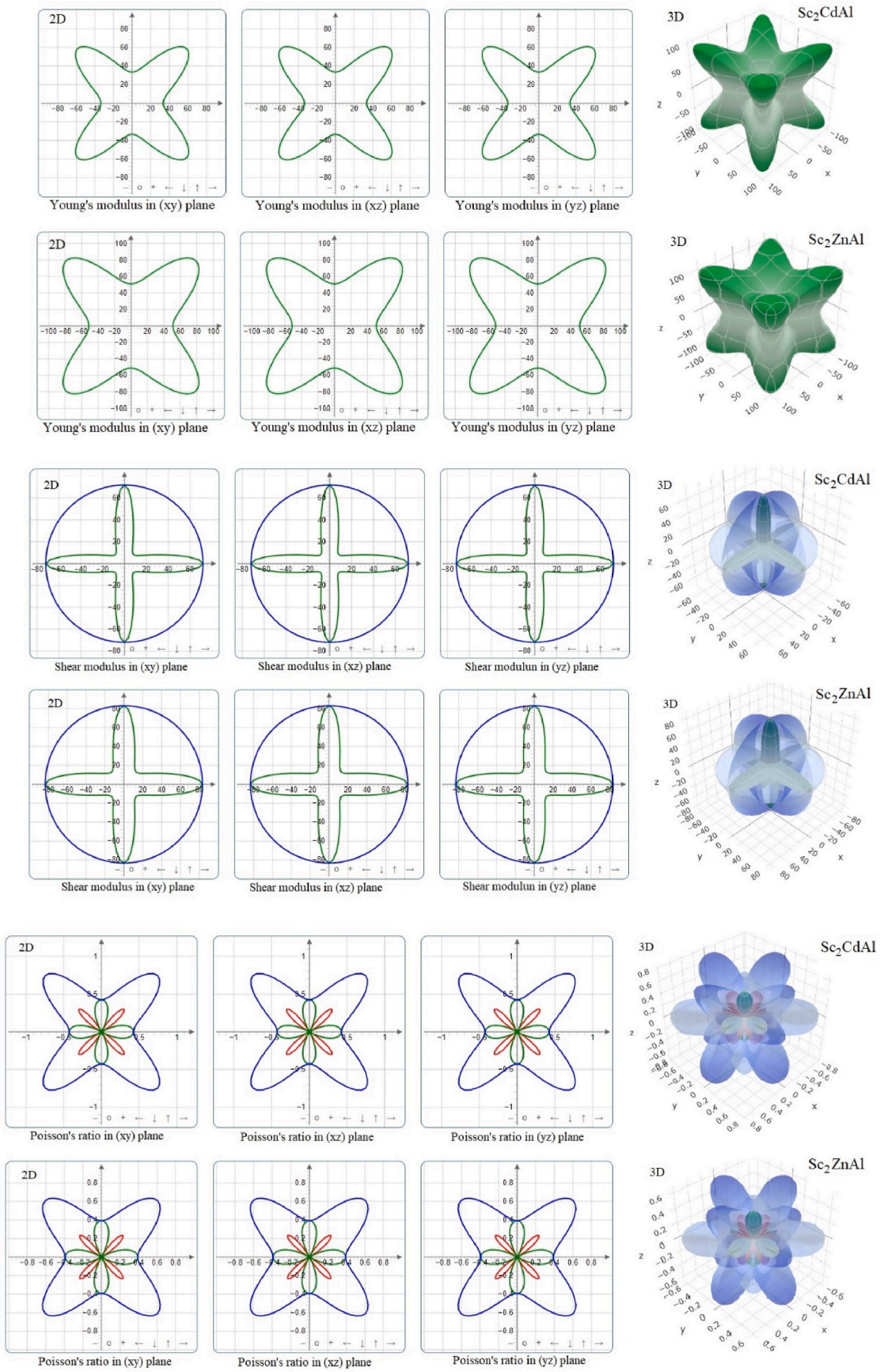

Fig. 2. 2D and 3D curves of Young modulus, shear modulus and Poisson's ratio for Sc_2XAl (X = Cd and Zn) alloys.

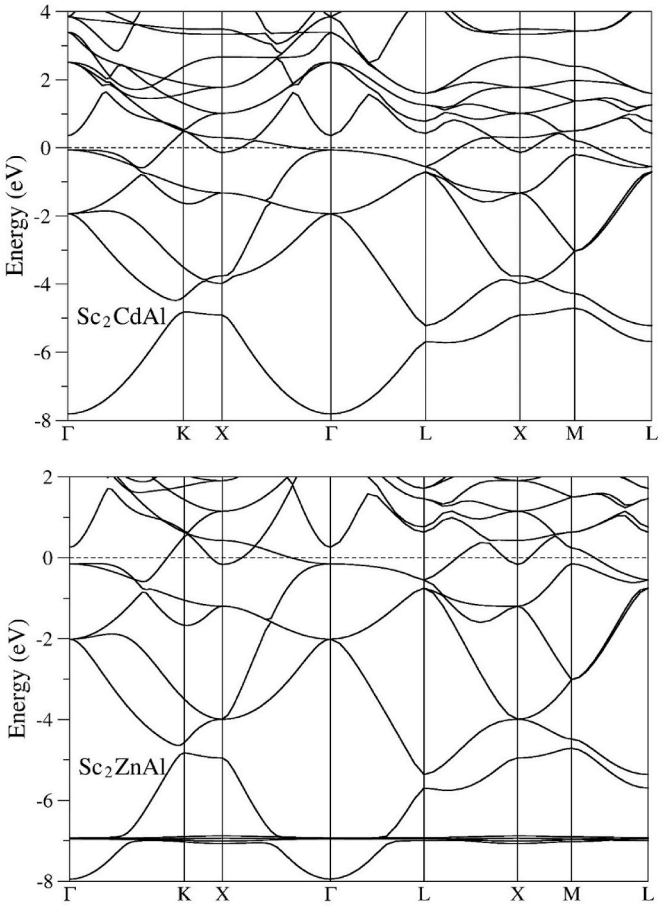

Fig. 3. Electronic band spectrum of Sc_2XAl (X = Cd and Zn) alloys.

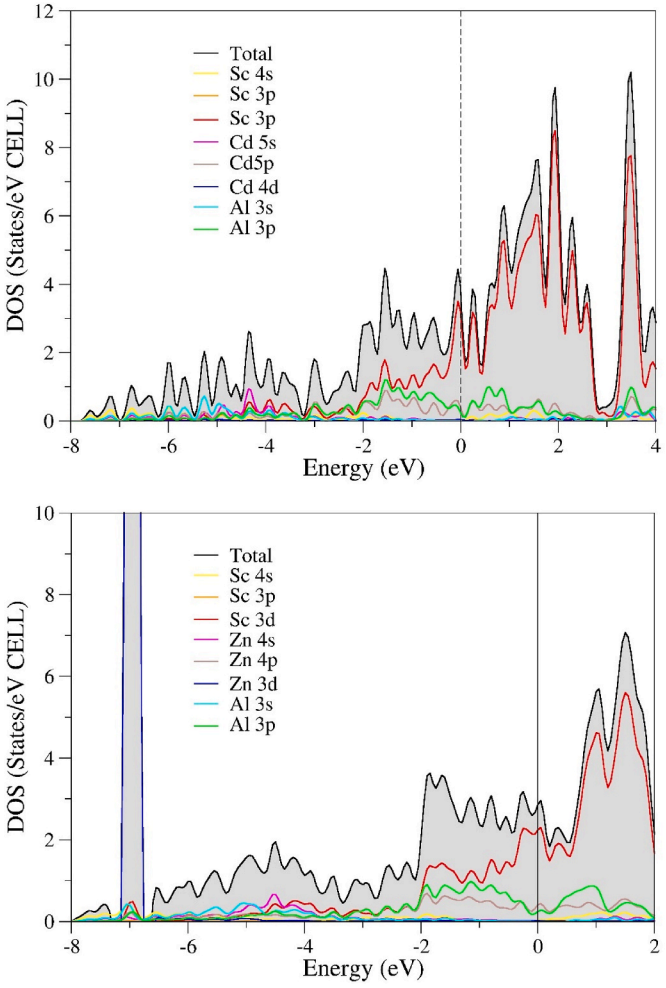

Fig. 4. Total and partial density of states for Sc_2XAl (X = Cd and Zn) alloys.

the evaluated value is 0.817 and 0.750, respectively, we can conclude that bond bending and stretching are possible in all alloys. As the value approaches 1, bond bending outpaces bond tension.

$$H_\nu = \frac{(1-2\nu)E}{6(1+\nu)} \tag{9}$$

Microhardness parameter H_ν also provide information about hardness of the materials when they are compared with other materials. Both alloys have very lower values like 5.512 and 7.980 GPa (Sc_2CdAl and Sc_2ZnAl, respectively) than diamond which is the hardest material known with 96 GPa.

3.1. Anisotropy

Crystals' mechanical characteristics are intrinsically anisotropic, with stress-strain responses varying depending on the crystallographic axis of interest. Solids with significant elastic anisotropy may tend to cause microcracks and mechanical failures under stress. Exposure of materials to stress causes microcracks that have the potential to expand and subsequently might cause mechanical failures such as material fracture. The elastic anisotropy factor (A) is determined from Equation (11). It is possible for the crystal to be isotropic when A is equal to 1 but for any value smaller or larger than 1 it indicates anisotropy.

$$A = \frac{2C_{44}}{C_{11} - C_{12}} \tag{11}$$

Predicted anisotropy factors for Sc_2CdAl and Sc_2ZnAl alloys are given in Table 2, and these values are less than one; This shows that the herein alloys studied are anisotropic. The detailed direction dependence analysis of the elastic anisotropy of the materials studied here is examined with 2D and 3D curves of Young's modulus, shear modulus and Poisson's ratio obtained using the ELATE program [40] and is presented in Fig. 2. In both materials examined, changes in Young's modulus, shear modulus and Poisson's ratios along the x, y and z directions can be seen in Fig. 2. Both materials exhibit anisotropic behavior considering the curves of Young's modulus, shear modulus and Poisson's ratios of because they deviate from the circular shape.

3.2. Electronic properties

Along the high symmetry directions occurring inside the Brillouin region, the calculated band structure was plotted to estimate the electronic properties of Sc_2XAl (X = Cd and Zn) in the $L2_1$ phase. These predicted band structures are presented in Fig. 3 in the direction of high symmetry directions. No band gap was detected at the Fermi level (EF) for the alloys in the $L2_1$ phase. Thus, this band character exhibits the metallic structure of the alloys studied. To understand the configurations of the band structure in more detail, the calculations were achieved for the total and partial density of states, as illustrated in Fig. 4. Our findings show that, because of an overlap in the density of states at the Fermi energy level, total and partial density of states confirm the metallic character already examined in the band structures. In addition, Sc-3d electrons contribute to showing the metallic nature of both alloys. We see that DOS is mainly associated with the 3 d-state of Sc; This implies that bonding states are predominantly present in the Sc atom in the region above the Fermi energy from −2 eV, and the contribution of Cd-d (Zn-d) states is located around −7 eV below the Fermi level for all

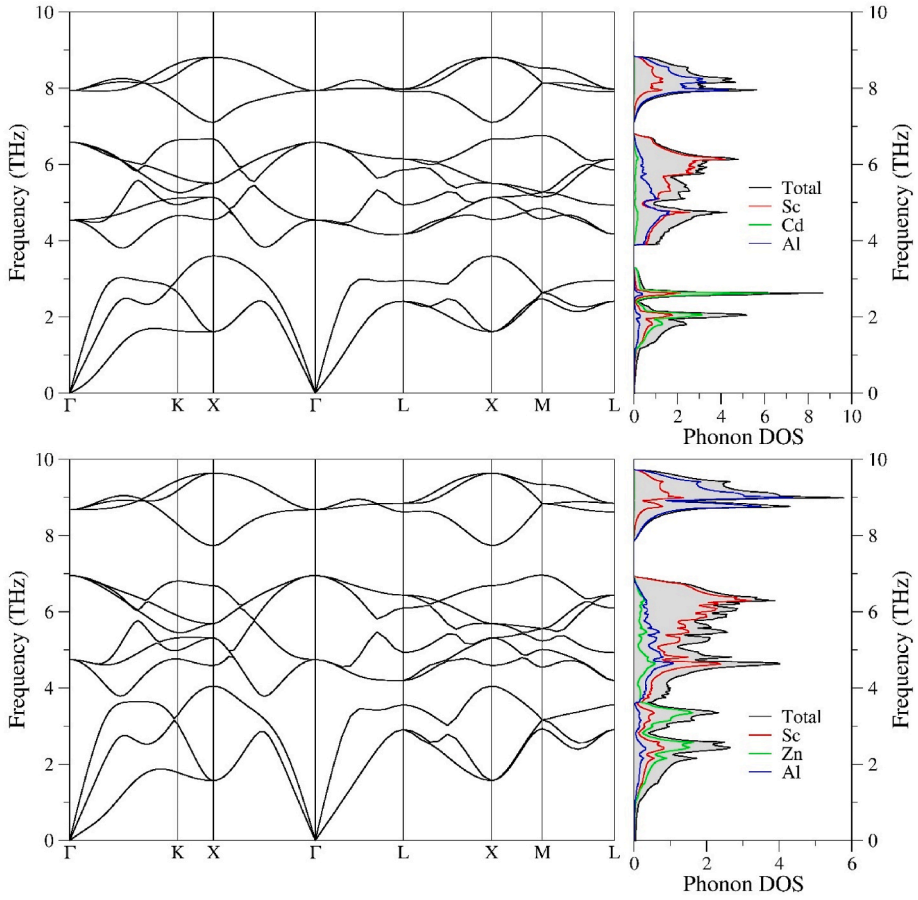

Fig. 5. Full phonon spectra and corresponding total and projected density of states curves for Sc_2XAl (X = Cd and Zn) alloys.

systems.

3.3. Phonon properties

Presented in Fig. 5 shows the predicted phonon dispersion relationship of Sc_2CdAl and Sc_2ZnAl full Heusler alloys. Calculations of the phonon dispersion relationship are performed using the quantum-espresso code. Since the unit cell of the herein considered alloys here in the $L2_1$ phase includes four atoms, it contains 12 phonon branches, three acoustic and nine optical. From the full phonon spectra of both alloys studied here, it can be said that both alloys are dynamically stable since there is no sign of imaginary branches in the phonon dispersions. The phonon dispersion curves point out that Sc_2CdAl the acoustic phonon modes and optical phonon modes are completely separated from each other, while for Sc_2ZnAl there is a partial overlap. On the other hand, in both alloys, the top optical phonon modes are separated from the other optical modes and a phonon band gap is present. Because the phonon band gaps only create a reflection from the surface and do not propagate sound, they may be used in a variety of applications, including sound filters and mirrors [41,42]. These kinds of qualities make the materials perfect for usage in mirrors and insulators. For a more detailed analysis of the full phonon spectrum, the phonon density of states (PDOS) corresponding to the full phonon spectrum is given in Fig. 5. The low-frequency phonon modes below about 4 THz are mainly dominated by Cd (Zn) atomic vibrations, while between 4 THz and 7 THz the middle-frequency branches arise from the vibration of slightly lighter Sc atoms. Thus, Al atoms, which have the lightest mass, also vibrate above 7 THz.

3.4. Thermodynamic properties

This study focused on investigating the thermodynamical properties of Sc_2XAl Heusler alloys at various temperatures using the framework of the Debye model quasi-harmonic method implemented in the Gibbs code. Lattice vibration, motion of molecules and phase transition have been calculated by the specific heat at constant volume C_v.

The calculation of the thermodynamical properties of Sc_2XAl at various temperatures has been done with the quasi-harmonic Debye approximation. In conclusion, in this approximation, the role of temperature and pressure on heat capacity, Debye temperature, enthalpy, entropy, and Gibbs free energy were found out (Fig. 6a-d). Vibrational free energy-temperature graph contributed to figure out the phase stability of the materials.

The Debye vibrational energy (Fig. 6a) and the Gibb's free energy (Fig. 6b) for both alloys show non-linear increase and non-linear decrease with increasing temperature. The zero value of entropy (Fig. 6c) obey the third law of thermodynamics between 0 K and 50 K. There is very little disorder among atoms, or, in other words, there are perfect crystals exist at the absolute zero temperature. Due to its nature, the increase in both temperature and the system's entropy causes a disorder. On the other hand, specific heat capacity of both alloys reaches to zero (Fig. 6d) with absolute zero temperature as in agreement with the Debye model. At low temperatures, the phonon contribution has the main influence on C_v curve while temperature up to about 300 K the specific heat capacity has under the effect of phonon thermal vibrations. Approaching the Dulong-Petit classical limit brought an anharmonic effect on the specific heat capacity. At the intermediate temperature between 100 and 300 K, the specific heat capacity depends on the atomic lattice vibrations.

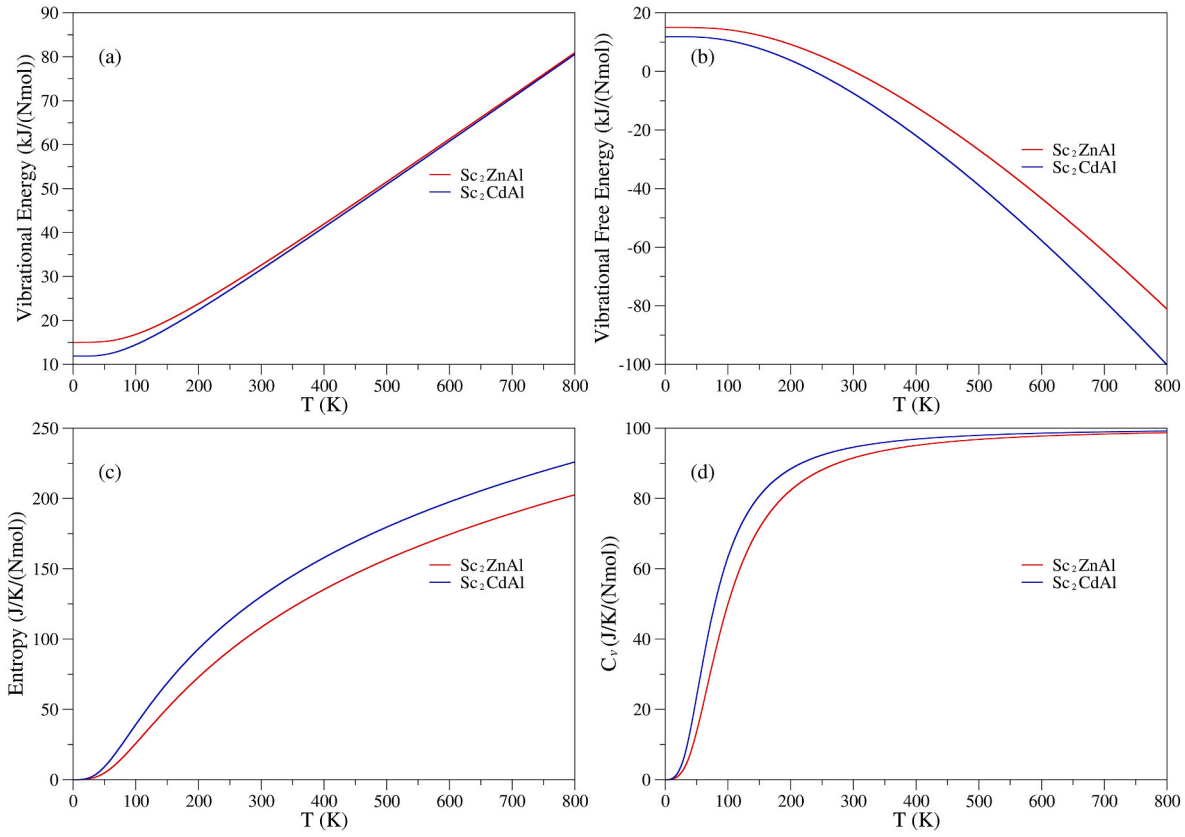

Fig. 6. The role of temperature on; a) vibrational energy, b) vibrational free energy, c) entropy, and d) heat capacity.

$$T_m = 553 + 5.91C_{44} \quad (10)$$

T_m shows the strength of the bonds holding the alloys' atoms together and how they behave against heat. The values from Table 2 point out the existence of strong bonds between the atoms of Sc_2CdAl (958.064K) and Sc_2ZnAl (1024.499K) which exhibit higher T_m values.

4. Conclusions

In this work, density functional theory based on GGA approximations was applied to the full Heusler alloys Sc_2CdAl and Sc_2ZnAl to understand their structural, elastic, electronic, thermodynamic, and phonon characteristics. The negative formation enthalpies obtained for both materials that are an important indicator of how mechanical stability works and in what level experimental synthesizability can be used to compare both results. Since the elastic constants after calculation comply with the Born stability criteria, the analysis shows that both materials exhibit mechanical stability at a satisfactory level. The calculated findings on mechanical properties exhibited that Sc_2CdAl alloy is ductile nature and Sc_2ZnAl is brittle manner. The elements in the alloys have chemical bonds that are connected mostly in the form of metallic bonds. It is also predicted that the alloys have anisotropic elasticity. The electronic band profile and density of states of Sc_2XAl (X = Cd and Zn) alloys demonstrate that they are metallic and non-magnetic. The dynamic properties of Sc_2XAl (X = Cd and Zn) such as phonon dispersion and partial densities of states were examined in lights of density functional perturbation theory. The phonon dispersion curves and partial densities of states for the materials confirm the dynamic stability of both alloys in the Full Heusler structure. Finally, due to do thermodynamic investigation, the vibrational free energy, internal free energy, entropy, and specific heat at constant volume C_v of the Sc_2CdAl and Sc_2ZnAl have been studied and analyzed across the temperature changes between 0K and 800K using the quasi-harmonic approximation. The herein results suggest the alloys as good candidates can easily be synthesized in practice for future practical thermoelectric applications.

CRediT authorship contribution statement

Nihat Arıkan: Supervision, Methodology, Data curation, Conceptualization. **Osman Örnek:** Visualization, Investigation. **Ahmet İyigör:** Writing – original draft, Validation, Software. **Murat Çanlı:** Writing – review & editing.

Declaration of competing interest

The authors declare that they have no known competing financial interests or personal relationships that could have appeared to influence the work reported in this paper.

Data availability

Data will be made available on request.

References

[1] V. Srivastava, N. Kaur, R. Khenata, S. Dar, Investigation of the electronic, magnetic, elastic, thermodynamic and thermoelectric properties of Mn_2CoCr Heusler compound A DFT-based simulation, J. Magn. Magn Mater. 513 (2020) 167107.
[2] K.M. Al-Masri, M.S. Abu-Jafar, M. Farout, D. Dahliah, A.A. Mousa, S.M. Azar, R. Khenata, Structural, elastic, electronic, and magnetic properties of full-heusler alloys Sc2TiAl and Sc2TiSi using the FP-lapw method, Magnetochemistry 9 (4) (2023) 108.
[3] M. Manzoor, D. Behera, R. Sharma, M.W. Iqbal, S.K. Mukherjee, R. Khenata, S. S. Alarfaji, H.A. Alzahrani, Investigation of the structural, mechanical, optoelectronic and, thermoelectric characteristics of cubic GeTiO3: an ab initio study, Matt. Today Comm 34 (2023) 105053.
[4] R. Moussa, Y. Djalab, M. Maache, R. Khenata, S. Bin-Omran, S.A. Rouf, M.W. Iqbal, A. Abdiche, W. Ahmed, M. Manzour, An investigation using DFT methods on the

electronic and optical properties, and mechanical behavior of the wurtzite ZnO1-xTex ternary alloy, Curr. Appl. Phys. 55 (2023) 82–92.
[5] A. Bedjaoui, D. Allali, M. Radjai, A. Bouhemadou, S.S. Essaoud, S. Bin-Omran, R. Khenata, Y. Al-Douri, Ab initio predictions of pressure-dependent structural, elastic, and thermodynamic properties of GaMF3 (M= Ca, and Sr) halide perovskites, Solid State Commun. 387 (2024) 115532.
[6] N. Arıkan, A. İyigör, A. Candan, Ş. Uğur, Z. Charifi, H. Baaziz, G. Uğur, Electronic and phonon properties of the full-Heusler alloys X_2YAl (X= Co, Fe and Y= Cr, Sc): a density functional theory study, J. Mater. Sci. 49 (2014) 4180–4190.
[7] Y. Han, Z. Chen, M. Kuang, Z. Liu, X. Wang, X. Wang, 171 Scandium-based full Heusler compounds: a comprehensive study of competition between XA and L21 atomic ordering, Results Phys. 12 (2019) 435–446.
[8] T. Graf, C. Felser, S.S. Parkin, Simple rules for the understanding of Heusler compounds, Prog. Solid State Chem. 39 (1) (2011) 1–50.
[9] B. Abdelkebir, Z. Charifi, H. Baaziz, T. Ghellab, R. Khenata, S. Bin-Omran, Iridium's influence on the structural, electronic and mechanical characteristics of ZrCo1-xIrxSb half-heusler alloys, Phys. B Condens. Matter 416166 (2024).
[10] Y.E. Krimia, R. Masroura, A. Jabara, S. Labidib, M. Bououdinac, M. Ellouzed, Results Phys. 18 (2020) 103252–103258.
[11] D. Vishali, R. John, Structural, electronic and magnetic properties of the Half-Heusler alloy CrZSi (Z= Sc, Ti), J. Cryst. Growth 583 (2022) 126556.
[12] K.M. Al-Masri, M.S. Abu-Jafar, M. Farout, D. Dahliah, A.A. Mousa, S.M. Azar, R. Khenata, Structural, elastic, electronic, and magnetic properties of full-heusler alloys Sc2TiAl and Sc2TiSi using the FP-lapw method, Magnetochemistry 9 (4) (2023) 108.
[13] S. Al, N. Arikan, A. Iyigör, Investigations of structural, elastic, electronic and thermodynamic properties of X_2TiAl Alloys: a computational study, Z. Naturforsch. 73 (9) (2018) 859–867.
[14] C. Wang, F. Casper, T. Gasi, V. Ksenofontov, B. Balke, G.H. Fecher, C. Felser, Y. Hwu, J. Lee, Structural and magnetic properties of Fe2CoGa Heusler nanoparticles, J. Phys. Appl. Phys. 45 (2012) 295001.
[15] A.K. Nayak, C. Shekhar, J. Winterlik, A. Gupta, C. Felser, Mn2PtIn: a tetragonal Heusler compound with exchange bias behavior, Appl. Phys. Lett. 100 (2012) 152404.
[16] L. Hao, R. Khenata, X. Wang, T. Yang, Ab Initio study of the structural, electronic, magnetic, mechanical and thermodynamic properties of full-Heusler Mn 2 CoGa, J. Electron. Mater. 48 (2019) 6222–6230.
[17] A. Iyigör, S. Al, N. Arikan, Density functional theory investigation on structural, mechanical, electronic and vibrational properties of Heusler alloys $AlXIr_2$ (X= Co, Cr, Cu, Fe and Zn), Chem. Phys. Lett. 806 (2022) 140052.
[18] S. Al, N. Arikan, S. Demir, A. Iyigör, Lattice dynamic properties of Rh2XAl (X= Fe and Y) alloys, Phys. B Condens. Matter 531 (2018) 16–20.
[19] T. Graf, C. Felser, S.S. Parkin, Simple rules for the understanding of Heusler compounds, Prog. Solid State Chem. 39 (2011) 1–50.
[20] M. Çanlı, E. Ilhan, N. Arıkan, First-principles calculations to investigate the structural, electronic, elastic, vibrational and thermodynamic properties of the full-Heusler alloys X2ScGa (X= Ir and Rh), Mater. Today Commun. 26 (2021) 101855.
[21] A.K. Nayak, M. Nicklas, S. Chadov, C. Shekhar, Y. Skourski, J. Winterlik, C. Felser, Large zero-field cooled exchange-bias in bulk Mn2PtGa, Phys. Rev. Lett. 110 (2013) 127204.
[22] A. Bouhemadou, O. Boudrifa, N. Guechi, R. Khenata, Y. Al-Douri, Ş. Uğur, B. Ghebouli, S. Bin-Omran, Structural, elastic, electronic, chemical bonding and optical properties of Cu-based oxides ACuO (A= Li, Na, K and Rb): an ab initio study, Comput. Mater. Sci. 81 (2014) 561–574.
[23] M. Hachemaoui, R. Khenata, A. Bouhemadou, A.H. Reshak, D. Rached, F. Semari, FP-APW+ lo study of the elastic, electronic and optical properties of the filled skutterudites CeFe4As12 and CeFe4Sb12, Curr. Opin. Solid State Mater. Sci. 13 (5–6) (2009) 105–111.
[24] A. Bouhemadou, R. Khenata, Ab initio study of structural phase stability and elastic properties of ScSb and YSb under pressure effect, Phys. Lett. 362 (5–6) (2007) 476–479.
[25] P. Giannozzi, S. Baroni, N. Bonini, M. Calandra, R. Car, C. Cavazzoni, R. M. Wentzcovitch, Quantum espresso: a modular and open-source software project for quantum simulations of materials, J. Phys. Condens. Matter 21 (39) (2009) 395502.
[26] P. Giannozzi, O. Andreussi, T. Brumme, O. Bunau, M.B. Nardelli, M. Calandra, S. Baroni, Advanced capabilities for materials modelling with Quantum ESPRESSO, J. Phys. Condens. Matter 29 (46) (2017) 465901.
[27] J.P. Perdew, K. Burke, M. Ernzerhof, Generalized gradient approximation made simple, Phys. Rev. Lett. 77 (18) (1996) 3865.
[28] W. Kohn, L.J. Sham, Self-consistent equations including exchange and correlation effects, Phys. Rev. 140 (4A) (1965) A1133.
[29] H.J. Monkhorst, J.D. Pack, Special points for Brillouin-zone integrations, Phys. Rev. B 13 (12) (1976) 5188.
[30] S. Baroni, P. Giannozzi, A. Testa, Green's-function approach to linear response in solids, Phys. Rev. Lett. 58 (18) (1987) 1861.
[31] S.A. Khandy, I. Islam, D.C. Gupta, R. Khenata, A. Laref, Lattice dynamics, mechanical stability and electronic structure of Fe-based Heusler semiconductors, Sci. Rep. 9 (1) (2019) 1475.
[32] A. Bouhemadou, R. Khenata, F. Zerarga, Ab initio study of the structural and elastic properties of spinels MgX2O4 (X= Al, Ga, In) under pressure, Eur. Phys. J. B 56 (2007) 1–5.
[33] A. Jain, S.P. Ong, G. Hautier, W. Chen, W.D. Richards, S. Dacek, S. Cholia, D. Gunter, D. Skinner, G. Ceder, K.A. Persson, Commentary: the Materials Project: a materials genome approach to accelerating materials innovation, Apl. Mater. 1 (1) (2013).
[34] J.E. Saal, S. Kirklin, M. Aykol, B. Meredig, C. Wolverton, Materials design and discovery with high-throughput density functional theory: the open quantum materials database (OQMD), J. Occup. Med. 65 (2013) 1501–1509.
[35] F. Mouhat, F.X. Coudert, Necessary and sufficient elastic stability conditions in various crystal systems, Phys. Rev. B 90 (22) (2014) 224104.
[36] M. Born, On the stability of crystal lattices, I, Math. Proc. Camb. Phil. Soc. 36 (2) (1940). Cambridge University Press.
[37] W. Voigt, Lehrbuch der kristallphysik:(mit ausschluss der kristalloptik), vol. 34, BG Teubner, 1910.
[38] A. Reuss, Berechnung der fließgrenze von mischkristallen auf grund der plastizitätsbedingung für einkristalle, ZAMM-Journal of Applied Mathematics and Mechanics/Zeitschrift für Angewandte Mathematik und Mechanik 9 (1) (1929) 49–58.
[39] R. Hill, The elastic behaviour of a crystalline aggregate, Proc. Phys. Soc. 65 (5) (1952) 349.
[40] R. Gaillac, P. Pullumbi, F.X. Coudert, ELATE: an open-source online application for analysis and visualization of elastic tensors, J. Phys. Condens. Matter 28 (27) (2016) 275201.
[41] N. Arikan, H.Y. Ocak, G. Dikici Yıldız, Y.G. Yıldız, R. Ünal, Investigation of the mechanical, electronic and phonon properties of X 2 ScAl (X= Ir, Os, and Pt) Heusler compounds, J. Kor. Phys. Soc. 76 (2020) 916–922.
[42] R.M. Hornreich, M. Kugler, S. Shtrikman, C. Sommers, Phonon band gaps, J. Phys. 7 (3) (1997) 509–519.